



openheart Predictors of post-TAVI conduction abnormalities in patients with bicuspid aortic valves

Giulia Esposito ^{1,2}, Niraj Kumar,^{2,3} Francesca Pugliese,^{2,4} Max Sayers,² Anthony WC Chow,² Simon Kennon,² Mick Ozkor,² Anthony Mathur,^{5,6} Andreas Baumbach,^{6,7} Guy Lloyd,² Aigerim Mullen,³ Andrew Cook,³ Michael Mullen ², Kush P Patel^{2,3}

► Additional supplemental material is published online only. To view, please visit the journal online (<http://dx.doi.org/10.1136/openhrt-2022-001995>).

To cite: Esposito G, Kumar N, Pugliese F, *et al.* Predictors of post-TAVI conduction abnormalities in patients with bicuspid aortic valves. *Open Heart* 2022;**9**:e001995. doi:10.1136/openhrt-2022-001995

GE and NK contributed equally.

Received 17 February 2022
Accepted 6 June 2022



© Author(s) (or their employer(s)) 2022. Re-use permitted under CC BY-NC. No commercial re-use. See rights and permissions. Published by BMJ.

For numbered affiliations see end of article.

Correspondence to
Dr Kush P Patel; kush.p.patel04@gmail.com

ABSTRACT

Objectives This study evaluates predictors of conduction abnormalities (CA) following transcatheter aortic valve implantation (TAVI) in patients with bicuspid aortic valves (BAV).

Background TAVI is associated with CA that commonly necessitate a permanent pacemaker. Predictors of CA are well established among patients with tricuspid aortic valves but not in those with BAV.

Methods This is a single-centre, retrospective, observational study of patients with BAV treated with TAVI. Pre-TAVI ECG and CT scans and procedural characteristics were evaluated in 58 patients with BAV. CA were defined as a composite of high-degree atrioventricular block, new left bundle branch block with a QRS >150 ms or PR >240 ms and right bundle branch block with new PR prolongation or change in axis. Predictors of CA were identified using regression analysis and optimum cut-off values determined using area under the receiver operating characteristic curve analysis.

Results CA occurred in 35% of patients. Bioprosthesis implantation depth, the difference between membranous septum (MS) length and implantation depth (δ MSID) and device landing zone (DLZ) calcification adjacent to the MS were identified as univariate predictors of CA. The optimum cut-off for δ MSID was 1.25 mm. Using this cut-off, low δ MSID and DLZ calcification adjacent to MS predicted CA, adjusted OR 8.79, 95% CI 1.88 to 41.00; $p=0.01$. Eccentricity of the aortic valve annulus, type of BAV and valve calcium quantity and distribution did not predict CA.

Conclusions In BAV patients undergoing TAVI, short δ MSID and DLZ calcification adjacent to MS are associated with an increased risk of CA.

INTRODUCTION

With a prevalence of 0.9%–2% in the general population, bicuspid aortic valves (BAV) represent the most common congenital cardiac anomaly.^{1–4} BAV have a stronger tendency than tricuspid aortic valves (TAV) to cause aortic stenosis (AS), which tends to develop earlier in life.^{5–7} Unique anatomical differences compared with TAV pose

WHAT IS ALREADY KNOWN ON THIS TOPIC

⇒ ECG, anatomical and procedural factors are associated with conduction abnormalities (CA) post-transcatheter aortic valve implantation in patients with tricuspid aortic valves.

WHAT THIS STUDY ADDS

⇒ Among patients with bicuspid aortic valves (BAV), short membranous septum (MS) length and implantation depth and device landing zone calcification adjacent to the MS are associated with an eightfold increased risk of CA. The quantity and distribution of valve calcification, eccentricity of the AV annulus or type of BAV were not associated with CA.

HOW THIS STUDY MIGHT AFFECT RESEARCH, PRACTICE OR POLICY

⇒ Larger studies examining the type of BAV and techniques to prevent CA are needed.

a challenge to transcatheter aortic valve implantation (TAVI) including larger aortic root dimensions, more eccentric annulus, effaced sinuses, longer and more asymmetrical leaflets, concomitant presence of aortopathy, shorter membranous septum (MS), heavier calcific burden and the presence of calcified raphe.^{3 8–11} The evolution of TAVI has enabled progressively younger and lower-risk populations to be treated.^{12 13} Patients with BAV have been excluded from pivotal TAVI trials. However, several observational studies have evaluated the safety and efficacy of TAVI in patients with BAV demonstrating lower procedural success and higher complication rates, especially when using early-generation devices.^{14–17}

Among these procedural complications is a significant incidence of conduction abnormalities (CA) leading to permanent pacemaker implantation (PPMI). A meta-analysis showed rates of new PPM, in BAV and TAV, respectively, of 17% and 26% using

early-generation bioprosthesis, and 9.9% and 8.6% using new-generation bioprosthesis.¹⁸ Studies among patients with TAV have demonstrated ECG, anatomical and procedural factors that increase the risk of CA with TAVI.^{19,20} However, there is a lack of data regarding these characteristics in patients with BAV undergoing TAVI. This study examined the predictive role of pre-TAVI CT-based anatomical characteristics and peri-TAVI procedural characteristics associated with post-TAVI CA.

METHODS

Study population

This retrospective, observational study included consecutive patients who underwent a TAVI for severe AS between January 2018 and December 2020 at a single centre, with a diagnosis of BAV (online supplemental figure 1). All patients underwent discussion at a multi-disciplinary team meeting to evaluate the indication, type and feasibility of valve replacement. TAVI was deemed to be the preferred treatment strategy in these patients. Patients with a BAV who were treated medically or surgically were not included in this study.

Patient and public involvement

Patients and the public were not involved in the design and conduct of this study.

Clinical investigations

All CT scans were performed on a Somatom FORCE scanner (Siemens Healthineers, Erlangen, Germany). The TAVI evaluation CT protocol involves a topogram, calcium score, timing bolus, gated CT coronary angiogram acquired retrospectively, and a FLASH whole-body scan (lung apices down to the lesser trochanters). The total volume of Omnipaque 300 (iohexol) contrast (GE Healthcare, Chicago, Illinois) was fixed at 90 mL (including a 10 mL timing bolus).

All transthoracic echocardiograms were performed by British Society of Echocardiography (BSE) accredited physiologists pre-TAVI and post-TAVI. Valvular and myocardial structure and function were analysed based on BSE guidance.²¹

A 12-lead ECG was performed pre-TAVI and at several time points post-TAVI before the patient was discharged.

TAVI Procedure

All TAVIs were performed at single tertiary cardiac centre. Patients underwent pre-TAVI clinical investigations that included a CT scan, ECG and transthoracic echocardiogram. All patients were discussed at a multi-disciplinary team meeting to evaluate their appropriateness for TAVI. Standard implantation techniques were used, with the choice of bioprosthesis left to the treating cardiologist. Patients have continuous ECG monitoring in the first 24 hours post-TAVI. This period is extended if significant CA are detected. Thereafter, patients have a daily ECG including on the day of discharge. ECGs were used to determine new CA that persisted until PPMI or

discharge. Those that developed indications for PPMI had the device implanted during the same admission. The decision to do so was made by the structural intervention and electrophysiology teams, in conjunction with the patient.

Data collection

Demographic, clinical and procedural data were collected prospectively onto a local database. Multivessel coronary artery disease was defined as more than one major coronary artery with a stenosis >50% or left main stem stenosis >50%. Patients were considered frail if they had a Rockwood clinical frailty score >5. The pre-TAVI and post-TAVI (pre-discharge) 12 lead ECG were compared, and any new CA was identified. BAV morphology was defined by the Siever's classification using CT.¹ The pre-TAVI CT was used to measure the following variables:

1. Diameters of the aortic valve (AV) annulus, sinus of Valsalva, sinotubular junction and ascending aorta.
2. Area of the AV annulus.
3. MS length
4. Valve calcification (measured by Agatston score and calcium volume).
5. Calcium distribution (see online supplemental figure 1).
6. Presence of calcium in device landing zone (DLZ) of the left ventricular outflow tract (LVOT)
7. Aorto-annular angle.

CT image analysis

All analyses were performed using a Syngo Via platform (Siemens Healthineers, Erlangen, Germany) by two observers independently. An average of these two results was used for analysis. Where a discrepancy >10% between measurements was noted, the case was reanalysed by both observers and a third observer together until a measurement was agreed on. Using multiplanar reconstructions (MPR), cross-sectional images were used to calculate diameter and area measurements. The Agatston scores and valve calcium volume were calculated using a Hounsfield threshold of 130 HU and a non-contrast sequence. Due to the heterogeneity in BAV morphologies (number of leaflets, number of raphe, site of raphe) demarcation of calcification according to cusp becomes challenging. Instead, given that conduction tissue in the septum is an important anatomical landmark for CA, we opted for a standardised method to calculate calcium distribution according to its relationship with the MS. Calcium distribution was calculated as any calcification involving the valve itself, based on whether it was adjacent to or opposite the MS, rather than according to the cusp, thereby providing consistency in measurements. This was determined by dividing the AV in two based on the position of the MS—a virtual line that is 30°–45° to the anterior–posterior axis of the body and often follows the commissure between the left and right coronary cusp (RCC) and cuts through the non-coronary cusp (NCC) (online supplemental figure 1). In patients with type 0

Table 1 Baseline characteristics compared between patients with and without CA

Variables	No conduction abnormality (n=38)	Conduction abnormality (n=20)	P value
Demographics			
Age (years)	79 (71–85)	79.5 (68–84)	0.812
Male gender	21 (55%)	12 (60%)	0.729
Height (cm)	158 (153–167)	164 (156–172)	0.191
Weight (kg)	71.7±16.1	80.6±15.2	0.078
Logistic EuroSCORE	7.5 (5.5–11.9)	5.5 (2.1–10.7)	0.197
Comorbidities			
eGFR (mL/min/1.73 m ²)	58.5±17.7	60.2±16.5	0.724
Diabetes	8 (21%)	4 (20%)	0.925
Hypertension	23 (60%)	12 (60%)	0.969
Pulmonary disease	11 (29%)	0 (0%)	0.008
Previous stroke	4 (11%)	2 (10%)	1
Previous myocardial infarction	6 (16%)	1 (5%)	0.403
Multivessel CAD	4 (11%)	2 (10%)	1
Frailty	3 (8%)	2 (10%)	1
Pre-TAVI echocardiography			
AV maximum velocity (m/s)	3.4±1.2	3.6±1.0	0.494
AV peak gradient (mm Hg)	61.0±30.2	60.1±24.3	0.927
AV mean gradient (mm Hg)	34.5±20.8	33.3±15.3	0.837
LVEF (%)	53 (38–59)	55 (39–63)	0.975
TAPSE (cm)	2.20±0.62	1.93±0.51	0.154
Bicuspid valve morphology			
BAV morphology (Sevier's classification)	Type 0 (AP)=4 (11%)	Type 0 (AP)=6 (30%)	0.288
	Type 0 (lat)=8 (21%)	Type 0 (lat)=1 (5%)	
	Type 1 (L-R)=20 (53%)	Type 1 (L-R)=10 (50%)	
	Type 1 (R-N)=3 (8%)	Type 1 (R-N)=1 (5%)	
	Type 1 (N-L)=2 (5%)	Type 1 (N-L)=2 (10%)	
	Type 2 (R-N)=1 (3%)	Type 2 (R-N)=0 (0%)	
Pre-TAVI CT analysis			
Calcium score (adjacent to MS)	1880 (1073–2605)	2092 (1232–4075)	0.421
Calcium volume (adjacent to MS) (mm ³)	1495 (858–2051)	1658 (961–3223)	0.401
Calcium score (opposite the MS)	1056 (591–1560)	796 (570–1603)	0.592
Calcium volume (opposite the MS) (mm ³)	837 (472–1242)	623 (456–1283)	0.61
Total valve calcium score	3117 (2042–3971)	2744 (1920–5956)	0.924
Total valve calcium volume (mm ³)	2477 (1646–3150)	2167 (1525–4735)	0.91
Aortic annulus diameter average (cm)	2.49±0.31	2.56±0.36	0.46
Eccentricity Index (cm)	0.78 (0.73–0.87)	0.78 (0.75–0.86)	1
Aortic annulus area (cm ²)	4.87±1.17	5.07±1.39	0.921
Sinus of valsalva diameter average (cm)	3.51±0.44	3.41±0.59	0.581
Sinotubular junction diameter average (cm)	3.30±0.43	3.15±0.63	0.534
Ascending aorta diameter average (cm)	3.77±0.44	3.91±0.58	0.284
Membranous septum depth (mm)	6.0 (5.0–8.4)	5.8 (4.5–7.3)	0.441
Aortic-annular angulation (degrees)	160.1±8.4	160.0±12.0	0.966
Pre-TAVI ECG			

Continued

Table 1 Continued

Variables	No conduction abnormality (n=38)	Conduction abnormality (n=20)	P value
Left axis deviation	3 (8%)	1 (5%)	1.000
First degree heart block	10 (26%)	1 (5%)	0.049
Right bundle branch block	2 (5%)	0 (0%)	0.54

Data are presented as mean±SD, median (IQR or number (percentage)).

AP, anterior–posterior; AV, aortic valve; BAV, bicuspid aortic valve; CA, conduction abnormalities; CAD, coronary artery disease; eGFR, estimated glomerular filtration rate; L, left; LVEF, left ventricular ejection fraction; MS, membranous septum; N, non-coronary; R, right; TAPSE, tricuspid annular planar systolic excursion.

BAV, this division was estimated based on the anatomical relationship between both atria and ventricles. Both Agatston score and calcium volume in mm³ were calculated. From the contrast enhanced MPR images, calcium in the DLZ of the LVOT was noted as being present or absent within the half adjacent to or opposite to the MS. Aortic annular eccentricity was calculated as the ratio between the smallest and largest diameter of the AV annulus. MS length was measured using the computerised measurement tool on Syngo Via on a contrast-enhanced coronal view using a previously described methodology.¹⁹ The MS was defined as the length of the thinnest portion of the septum, along the LVOT, from the AV annulus plane of the NCC to the boundary of the muscular interventricular septum. The aortoannular angle was measured as the angle between the longitudinal planes of the AV annulus and a point 4 cm distally in the aorta. The longitudinal plane was identified as a perpendicular line to the AV annulus and the cross section of the aorta 4 cm distal to the AV annulus. All the measurements above were determined using pre-TAVI CT scans.

Fluoroscopy image analysis

The depth of device implantation was measured using the procedural fluoroscopic image. This was determined at the time of the aortogram and comprised the distance from the AV annulus to the deepest part of the TAVI prosthesis within the left ventricle—a methodology proven to be reliably similar to CT determined implantation depth.²² The difference between MS length and implantation depth (δ MSID) was calculated to demonstrate the placement of the device relative to the MS.

Study endpoint

The primary endpoint was new post-TAVI CA defined as either new high degree atrioventricular block (complete or second degree heart block), new onset left bundle branch block with a QRS duration >150ms or PR interval >240ms, pre-existing right bundle branch block (RBBB) with new PR prolongation or change in axis, as observed during the post-TAVI period prior to hospital discharge. This definition was based on current guidelines.²³

Table 2 Univariate analysis for CA including CT based pre-TAVI variables and peri-TAVI implantation depth

Variable	Univariate analysis			P value
	OR	95% CI for OR		
		Lower limit	Upper limit	
DLZ calcium opposite to MS	2.872	0.809	10.192	0.103
DLZ calcium adjacent to MS	3.938	1.240	12.507	0.020
Calcium score adjacent to MS	1.000	0.999	1.000	0.712
Calcium score opposite to MS	1.000	1.000	1.001	0.203
Total AV calcium score	1.000	1.000	1.000	0.468
MS depth	0.910	0.727	1.138	0.408
Implantation depth	1.215	1.002	1.474	0.048
δ MSID	0.835	0.703	0.991	0.039
Eccentricity Index	0.621	0.002	157.041	0.866
Pre-TAVI balloon dilatation	2.800	0.899	8.717	0.076
Post-TAVI balloon dilatation	2.000	0.364	10.980	0.425

AV, aortic valve; CA, conduction abnormalities; DLZ, device landing zone; MS, membranous septum; TAVI, transcatheter aortic valve implantation; δ MSID, difference between membranous septum depth and implantation depth.

NO FIGURE FOUND **Figure 1** Predictors of CA in TAVI patients with bicuspid aortic valve stenosis. The figure illustrates the measurements of the MS, implantation depth and the difference between the two (δ MSID). It also illustrates the anatomical relationship between the TAVI bioprosthesis and the conduction tissue. Device landing zone calcification adjacent to the MS can be seen in red. δ MSID—difference between the MS depth and implantation depth; AUC, area under the curve; CA, conduction abnormalities; δ MSID, MS length and implantation depth; MS, membranous septum; PPMI, permanent pacemaker implantation ROC, receiver operating characteristic; TAVI, transcatheter aortic valve implantation.

Statistical analysis

Normality of continuous variables was evaluated using the Shapiro-Wilk test and presented using the mean \pm SD for parametric variables and median (IQR) for non-parametric variables. Frequencies are presented as number (percentage). Patients were divided according to whether they developed CA post-TAVI or not. Data were compared between these cohorts using a Student's t-test for parametric data, Mann-Whitney U test for non-parametric data, χ^2 or Fisher's exact test for frequencies as appropriate and for the distribution of calcification, the Wilcoxon signed-rank test. Univariate logistic regression was used to assess the association between various CT-derived and procedural variables and CA. Those that were significant were included into a multivariate regression model along with first degree heart block (an established predictor of CA). Area under the receiver operating characteristic curve was used to test the diagnostic ability of significant continuous variables, with the Youden's index used to identify optimal cut-off values. A new model was created using a composite of significant predictors to quantify their impact on CA. A two-sided $p < 0.05$ was considered statistically significant. All analysis were performed using SPSS version V.28.0 (SPSS). Data are not available for this study due to confidentiality reasons.

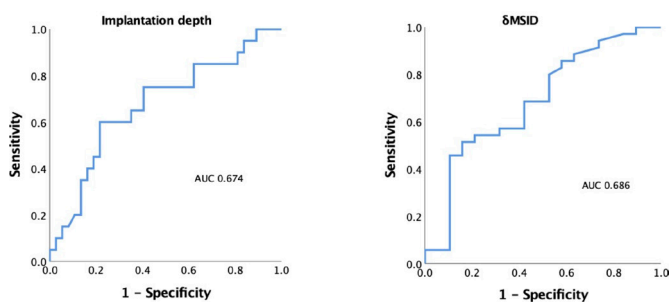


Figure 2 ROC curve analysis for CA for δ MSID and implantation depth. δ MSID—difference between MS depth and implantation depth.

RESULTS

Baseline characteristics

A total of 1856 patients had a TAVI during the study period, of which 58 patients had BAV and were included in this study, age 76.0 \pm 9.8 years, 57% male and Logistic EuroSCORE 6.5 (4.2–11.4). 20 patients (34.5%) developed CA, of which 9 patients required a PPM. Patients were divided according to presence or absence of CA and baseline characteristics were compared between the two cohorts (table 1). Overall, demographics, comorbidities (with the exception of pulmonary disease), echocardiographic and ECG findings were similar between both cohorts at baseline. Calcium distribution adjacent to versus opposite the MS was compared for the entire study population—calcium score: 974 (590–1581) vs 2020 (1129–2719) respectively; $p < 0.001$, respectively, and calcium volume: 789 (470–1249) vs 1595 (911–2167) mm³, respectively; $p < 0.001$.

TAVI procedure

The type of TAVI bioprosthesis used was similar between those with and without CA ($p = 0.266$). All patients had transfemoral access. 3 patients in each cohort had self-expandable valves implanted with the majority of valves being balloon-expandable (online supplemental table 1).

Implantation depth of the TAVI bioprosthesis in patients without compared with those with CA was 5.79 \pm 2.89 mm vs 7.49 \pm 3.05 mm; $p = 0.042$, respectively. δ MSID was 1.03 \pm 3.69 vs -1.32 \pm 3.85 mm; $p = 0.032$, respectively. The average length of stay post-TAVI was 4.1 \pm 6.0 days.

Predictors of CA

Univariate logistic regression for CA was performed on pre-TAVI CT based variables and peri-TAVI implantation depth (table 2). DLZ calcification adjacent to the MS, δ MSID and TAVI implantation depth demonstrated significant association with CA (figure 1).

Using ROC curve analysis, the AUC for implantation depth and δ MSID was 0.674 and 0.686, respectively (figure 2). The optimal cut-off for implantation depth and δ MSID was identified as 7.05 mm and 1.25 mm, respectively.

The diagnostic accuracy of these parameters was calculated using these cut-offs. Deep implantation demonstrated a high specificity (78%), but low sensitivity (60%), while low δ MSID demonstrated high sensitivity (84%) and low specificity (51%) (table 3).

Composite models for CA

Regression models were created incorporating the composite of DLZ calcification adjacent to the MS and the newly identified cut-offs for implantation depth (model 1) and δ MSID (model 2) separately. Model 1 demonstrated an adjusted OR for CA: 11.9, 95% CI 2.0 to 70.9; $p = 0.006$. Model 2 demonstrated an adjusted OR of 8.79, 95% CI 1.88 to 41.00; $p = 0.01$ (table 4).

Compared with patients without both a low δ MSID and DLZ calcification adjacent to the MS, those with

Table 3 Diagnostic accuracy of parameters

Parameter	Sensitivity	Specificity	PPV	NPV
DLZ calcification adjacent to MS	55%	76%	55%	76%
Deep implantation	60%	78%	60%	78%
low δ MSID	84%	51%	48%	86%
low δ MSID and DLZ calcification adjacent to MS	47%	91%	75%	76%
Deep implantation and DLZ calcification adjacent to MS	40%	95%	80%	74%

Deep implantation defined as >7.05 mm below the AV annulus. Low δ MSID defined as <1.25 mm.
DLZ, device landing zone; MS, membranous septum; NPV, negative predictive value; PPV, positive predictive value; δ MSID, difference between membranous septum and implantation depth.

only a low δ MSID or only DLZ calcification adjacent to the MS did not demonstrate an increased risk of CA. Only the combination of both factors demonstrated increased risk; unadjusted OR 36, 95% CI 3.193 to 405.897; $p=0.004$ (online supplemental table 2).

DISCUSSION

This study examined anatomical factors associated with post-TAVI CA in a BAV population. Our findings demonstrate that CA are associated with (1) deeper TAVI implantation, particularly in the presence of a short MS length and (2) presence of calcium in the DLZ adjacent to the MS. The composite of both factors is strongly predictive of CA. Lastly, the quantity and distribution of valve calcification, the eccentricity of the AV annulus or the type of BAV does not influence CA post-TAVI.

Although recent PPM rates have reduced with greater experience and improved technology,¹⁸ PPMI continues to place a significant burden on TAVI

patients. Pacing in TAVI is associated with reduced improvement in left ventricular ejection fraction and increased rates of heart failure hospitalisation.²⁴ Additionally, TAVI indications are expanding to include younger patients who will live longer—implying that more PPM device revisions will be required.²⁵ Therefore, identifying patients at increased risk of CA and taking precautions to reduce this risk is important. This is particularly the case for patients with BAV, who tend to develop complications at a younger age than those with TAV. Previous studies evaluating CA post-TAVI have actively excluded patients with BAV.^{26–28}

Our findings have important clinical implications for patients with BAV. Those with both DLZ calcification adjacent to the MS and a low δ MSID have over an eightfold increased risk of developing CA. Our findings also suggest that having just one of these risk factors may not significantly increase the risk of CA (online supplemental table 2). Pathophysiologically, this implies that for the development of CA, the TAVI bioprosthesis needs to be at a certain anatomical position in order to exert a radial force on adjacent calcification that would impinge on the atrioventricular conduction tissue. We identified an implantation depth of 7.05 mm and a δ MSID of 1.25 mm as the optimum cut-off values for prediction of post-TAVI CA. Similarly, another study in TAV patients, proposed similar cut-off values for implantation depth, ranging from 6.3 to 7.0 mm, depending on the type of TAVI bioprosthesis used.²⁹

Some studies conducted in TAV patients have found a shorter MS depth to be an independent predictor of post-TAVI CA and, thus, PPMI,^{19 26} but our study and that of Tretter *et al* did not.²⁷ There are several possible reasons that can explain this discrepancy. The location of the atrioventricular node is variable within the triangle of Koch and subsequently affects the location of the Bundle of His.³⁰ Additionally, the depth of the conduction tissue within the muscular ventricular septum and the force exerted by the TAVI bioprosthesis on this tissue is likely to vary.²⁷ These variations suggest that the susceptibility of the conduction tissues to impingement by a TAVI bioprosthesis may vary between populations. Within the BAV population,

Table 4 Multivariate regression models for conduction abnormalities

For conduction abnormalities				
Variable	OR	95% CI for OR		P value
		Lower limit	Upper limit	
Model 1				
Deep implantation and DLZ calcification adjacent to MS	11.93	2.01	70.95	0.006
1HB	0.14	0.01	1.40	0.094
Model 2				
Low δ MSID and DLZ calcification adjacent to MS	8.79	1.88	41.00	0.01
1HB	0.16	0.02	1.56	0.12

Deep implantation defined as >7.05 mm below the AV annulus. Low δ MSID defined as <1.25 mm.
AV, aortic valve; DLZ, device landing zone; 1HB, first degree heart block; MS, membranous septum; δ MSID, difference between membranous septum and implantation depth.

implantation depth and the subsequent δ MSID appear to be more important than MS depth.

A study among TAV patients demonstrated greater LCC calcification as a predictor of post-TAVI CA requiring PPMI.³¹ This finding can be explained by the anatomical location of the atrioventricular conduction tissue within the interleaflet fibrous triangle that separates the NCC from the RCC and opposite the LCC.³² More calcification of the LCC may potentially push the TAVI bioprosthesis towards the atrioventricular conduction axis, disturbing the bundle of His. BAV valves are known to be heavier, suggesting more calcification and fibrosis, compared with TAV,³³ with calcification described as asymmetrical and most commonly affecting the fused raphe and LCC.³⁴ In line with this, our findings demonstrated greater calcification opposite the MS. However, contrary to previous findings in TAV,³¹ this asymmetrical distribution of calcification was not associated with CA in patients with BAV.

Conversely, we found DLZ calcium adjacent to the MS had a significant impact on CA, a finding similar to a previous study among TAV patients.²⁶ The most plausible explanation for this, is that the radial force exerted by the bioprosthesis impinges the calcium onto the atrioventricular conduction tissue. Our study did not find any difference in CA between the different BAV morphologies, or due to aortic annular eccentricity.

Study limitations

This study is limited by its population size—58 patients, of which 20 suffered from post-TAVI CA. Consequently, this restricted our multivariate models to two covariates. The study population was derived from a TAVI cohort which is older and at higher surgical risk, limiting its generalisability to other patients with BAV. We predominantly used balloon expandable valves. Oversizing of valves was not measured in this study and has been shown to be an important determinant of post-TAVI CA.²² Additionally, we had a predominance of type 0 and type 1 (L-R) within our population. Larger studies need to evaluate whether certain morphologies increase the risk for CA. Pre-TAVI RBBB and self-expanding valves were not well represented in this population—two and six patients, respectively. Therefore, the lack of association between these variables and CA should not be interpreted as unimportant factors in the BAV population. Defining the AV annulus in order to measure implantation depth and MS depth can be challenging, especially in patients with type 0 BAV as only 2 cusp edges are available. However, by using three independent observers to analyse the data, we minimised the risk of inaccuracies. We did not consider post-discharge CA or PPMI as part of the endpoints, which can occur among TAVI patients. However, majority of CA do take place during the immediate post-TAVI period, implying that most events would have been captured in this study.

CONCLUSIONS

In patients with BAV undergoing TAVI, low δ MSID and DLZ calcification adjacent to the MS are associated with an increased risk of CA. The quantity and distribution of valve calcification, eccentricity of the AV annulus or type of BAV were not associated with CA.

Author affiliations

¹King's College London Faculty of Life Sciences and Medicine, London, UK

²Cardiology, Barts Health NHS Trust, London, UK

³University College London Institute of Cardiovascular Science, London, UK

⁴Centre for Advanced Cardiovascular Imaging, Queen Mary University William Harvey Research Institute, London, UK

⁵Barts Health NHS Trust, London, UK

⁶Centre for Cardiovascular Medicine and Devices, Queen Mary University William Harvey Research Institute, London, UK

⁷Barts Heart Centre, Barts Health NHS Trust, London, UK

Twitter Michael Mullen @bartstrctural

Contributors GE and NK were first joint authors of this study. GE, NK, KPP, MM, AC and AM were involved in the genesis and design of this study. All authors contributed to the data collection, GE, NK, MS, FP and KPP were involved in the CT analysis. GE, NK and KPP were involved in the statistical analysis. GE, NK, MM and KPP were involved in writing the initial draft of this manuscript. All authors read, edited and approved the manuscript. KPP is the guarantor.

Funding FP has received research support from Siemens Healthineers. AWCC has received Research grant from Boston Scientific and Abbott. AM is employed by Abbott Medical UK. MM has received grants and personal fees from Edwards Lifesciences and personal fees from Abbott Vascular. KPP is funded by a British Heart Foundation clinical research training fellowship grant (FS/19/48/34523) and has an unrestricted research grant from Edwards Lifesciences.

Competing interests All authors have completed the ICMJE uniform disclosure form at www.icmje.org/coi_disclosure.pdf and declare: no support from any organisation for the submitted work; no financial relationships with any organisations that might have an interest in the submitted work in the previous three years; no other relationships or activities that could appear to have influenced the submitted work. FP has received research support from Siemens Healthineers. AWCC has received Research grant from Boston Scientific and Abbott. AM is employed by Abbott Medical UK. MM has received grants and personal fees from Edwards Lifesciences and personal fees from Abbott Vascular. KPP is funded by a British Heart Foundation clinical research training fellowship grant (FS/19/48/34523) and has an unrestricted research grant from Edwards Lifesciences.

Patient consent for publication Not applicable.

Ethics approval This study involves human participants and was approved by North West-Greater Manchester South Research Ethics Committee Reference number: 21/NW/0182The North West-Greater Manchester South Research Ethics Committee waived the need for informed consent given the retrospective, observational nature of the study.

Provenance and peer review Not commissioned; externally peer reviewed.

Data availability statement No data are available. Data for this study are not available for sharing due to confidentiality reasons.

Supplemental material This content has been supplied by the author(s). It has not been vetted by BMJ Publishing Group Limited (BMJ) and may not have been peer-reviewed. Any opinions or recommendations discussed are solely those of the author(s) and are not endorsed by BMJ. BMJ disclaims all liability and responsibility arising from any reliance placed on the content. Where the content includes any translated material, BMJ does not warrant the accuracy and reliability of the translations (including but not limited to local regulations, clinical guidelines, terminology, drug names and drug dosages), and is not responsible for any error and/or omissions arising from translation and adaptation or otherwise.

Open access This is an open access article distributed in accordance with the Creative Commons Attribution Non Commercial (CC BY-NC 4.0) license, which permits others to distribute, remix, adapt, build upon this work non-commercially,

and license their derivative works on different terms, provided the original work is properly cited, appropriate credit is given, any changes made indicated, and the use is non-commercial. See: <http://creativecommons.org/licenses/by-nc/4.0/>.

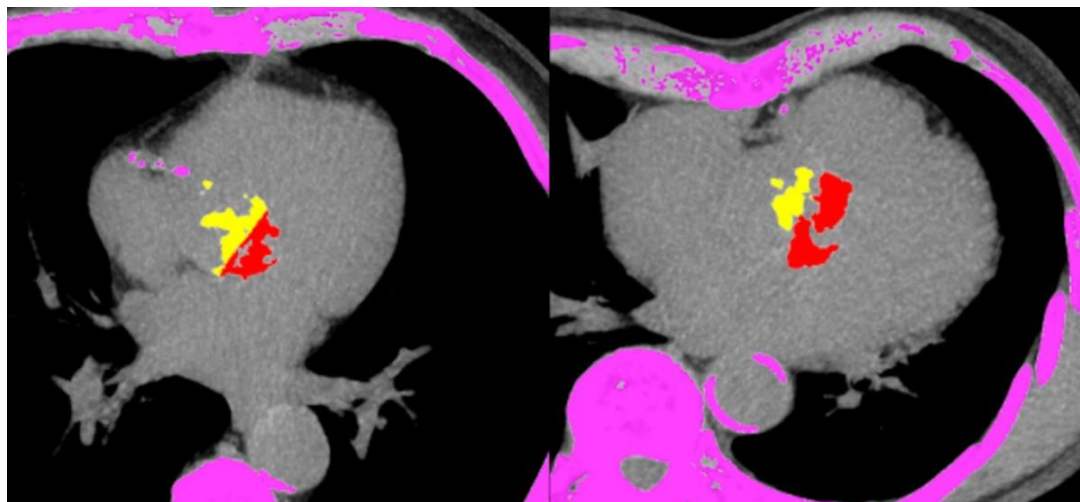
ORCID iDs

Giulia Esposito <http://orcid.org/0000-0001-5387-0147>

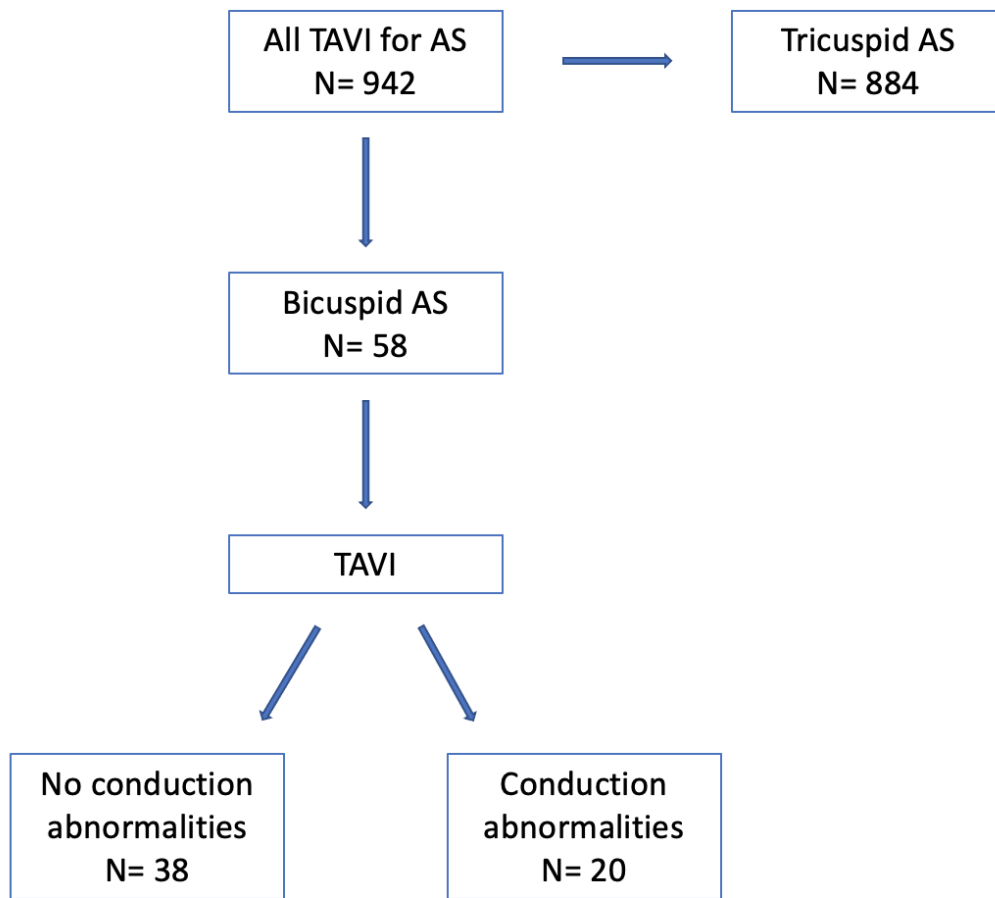
Michael Mullen <http://orcid.org/0000-0002-4911-3511>

REFERENCES

- Sievers H-H, Schmidtke C. A classification system for the bicuspid aortic valve from 304 surgical specimens. *J Thorac Cardiovasc Surg* 2007;133:1226–33.
- Fedak PWM, Verma S, David TE, et al. Clinical and pathophysiological implications of a bicuspid aortic valve. *Circulation* 2002;106:900–4.
- Siu SC, Silversides CK. Bicuspid aortic valve disease. *J Am Coll Cardiol* 2010;55:2789–800.
- Yoon S-H, Kim W-K, Dhoble A, et al. Bicuspid Aortic Valve Morphology and Outcomes After Transcatheter Aortic Valve Replacement. *J Am Coll Cardiol* 2020;76:1018–30.
- Carabello BA, Paulus WJ. Aortic stenosis. *Lancet* 2009;373:956–66.
- Lindman BR, Clavel M-A, Mathieu P, et al. Calcific aortic stenosis. *Nat Rev Dis Primers* 2016;2:16006.
- Beppu S, Suzuki S, Matsuda H, et al. Rapidity of progression of aortic stenosis in patients with congenital bicuspid aortic valves. *Am J Cardiol* 1993;71:322–7.
- Frangieh AH, Kasel AM. TAVI in Bicuspid Aortic Valves 'Made Easy'. *Eur Heart J* 2017;38:1177–81.
- Das R, Puri R. Transcatheter treatment of bicuspid aortic valve disease: imaging and interventional considerations. *Front Cardiovasc Med* 2018;5:91.
- Kawamori H, Yoon S-H, Chakravarty T, et al. Computed tomography characteristics of the aortic valve and the geometry of SAPIEN 3 transcatheter heart valve in patients with bicuspid aortic valve disease. *Eur Heart J Cardiovasc Imaging* 2018;19:1408–18.
- Hamdan A, Nassar M, Schwammenthal E, et al. Short membranous septum length in bicuspid aortic valve stenosis increases the risk of conduction disturbances. *J Cardiovasc Comput Tomogr* 2021;15:339–47.
- Mack MJ, Leon MB, Thourani VH, et al. Transcatheter aortic-valve replacement with a Balloon-Expandable valve in low-risk patients. *N Engl J Med Overseas Ed* 2019;380:1695–705.
- Popma JJ, Deeb GM, Yakubov SJ, et al. Transcatheter aortic-valve replacement with a self-expanding valve in low-risk patients. *N Engl J Med* 2019;380:1706–15.
- Hayashida K, Bouvier E, Lefèvre T, et al. Transcatheter aortic valve implantation for patients with severe bicuspid aortic valve stenosis. *Circ Cardiovasc Interv* 2013;6:284–91.
- Mylotte D, Lefevre T, Søndergaard L, et al. Transcatheter aortic valve replacement in bicuspid aortic valve disease. *J Am Coll Cardiol* 2014;64:2330–9.
- Bauer T, Linke A, Sievert H, et al. Comparison of the effectiveness of transcatheter aortic valve implantation in patients with stenotic bicuspid versus tricuspid aortic valves (from the German TAVI registry). *Am J Cardiol* 2014;113:518–21.
- Yoon S-H, Bleiziffer S, De Backer O, et al. Outcomes in Transcatheter Aortic Valve Replacement for Bicuspid Versus Tricuspid Aortic Valve Stenosis. *J Am Coll Cardiol* 2017;69:2579–89.
- Ueshima D, Nai Fovino L, Brener SJ, et al. Transcatheter aortic valve replacement for bicuspid aortic valve stenosis with first- and new-generation bioprostheses: a systematic review and meta-analysis. *Int J Cardiol* 2020;298:76–82.
- Hamdan A, Guetta V, Klempfner R, et al. Inverse relationship between membranous septal length and the risk of atrioventricular block in patients undergoing transcatheter aortic valve implantation. *JACC Cardiovasc Interv* 2015;8:1218–28.
- Maeno Y, Abramowitz Y, Kawamori H, et al. A highly predictive risk model for pacemaker implantation after TAVR. *JACC Cardiovasc Imaging* 2017;10:1139–47.
- Robinson S, Rana B, Oxborough D, et al. A practical guideline for performing a comprehensive transthoracic echocardiogram in adults: the British Society of echocardiography minimum dataset. *Echo Res Pract* 2020;7:G59–93.
- Guo Y, Zhou D, Dang M, et al. The predictors of conduction disturbances following transcatheter aortic valve replacement in patients with bicuspid aortic valve: a multicenter study. *Front Cardiovasc Med* 2021;8:757190.
- Glikson M, Nielsen JC, Kronborg MB, et al. 2021 ESC guidelines on cardiac pacing and cardiac resynchronization therapy. *Eur Heart J* 2021;42:3427–520.
- Chamandi C, Barbanti M, Munoz-Garcia A, et al. Long-Term Outcomes in Patients With New Permanent Pacemaker Implantation Following Transcatheter Aortic Valve Replacement. *JACC Cardiovasc Interv* 2018;11:301–10.
- Durko AP, Osnabrugge RL, Van Mieghem NM, et al. Annual number of candidates for transcatheter aortic valve implantation per country: current estimates and future projections. *Eur Heart J* 2018;39:2635–42.
- Maeno Y, Abramowitz Y, Kawamori H, et al. A highly predictive risk model for pacemaker implantation after TAVR. *JACC Cardiovasc Imaging* 2017;10:1139–47.
- Tretter JT, Mori S, Anderson RH, et al. Anatomical predictors of conduction damage after transcatheter implantation of the aortic valve. *Open Heart* 2019;6:e000972.
- Husser O, Pellegrini C, Kessler T, et al. Predictors of permanent pacemaker implantations and new-onset conduction abnormalities with the SAPIEN 3 Balloon-Expandable transcatheter heart valve. *JACC Cardiovasc Interv* 2016;9:244–54.
- Auffret V, Puri R, Urena M, et al. Conduction disturbances after transcatheter aortic valve replacement. *Circulation* 2017;136:1049–69.
- Anderson RH, Macias Y, et al. Variable arrangement of the atrioventricular conduction axis within the triangle of Koch. *JACC* 2020;6.
- Fujita B, Kütting M, Seiffert M, et al. Calcium distribution patterns of the aortic valve as a risk factor for the need of permanent pacemaker implantation after transcatheter aortic valve implantation. *Eur Heart J Cardiovasc Imaging* 2016;17:1385–93.
- Piazza N, de Jaegere P, Schultz C, et al. Anatomy of the aortic valvar complex and its implications for transcatheter implantation of the aortic valve. *Circ Cardiovasc Interv* 2008;1:74–81.
- Roberts WC, Janning KG, Ko JM, et al. Frequency of congenitally bicuspid aortic valves in patients ≥80 years of age undergoing aortic valve replacement for aortic stenosis (with or without aortic regurgitation) and implications for transcatheter aortic valve implantation. *Am J Cardiol* 2012;109:1632–6.
- van Rosendaal PJ, Kamperidis V, Kong WKF, et al. Comparison of quantity of calcific deposits by multidetector computed tomography in the aortic valve and coronary arteries. *Am J Cardiol* 2016;118:1533–8.

Supplementary figures

Supplementary figure 1: Non-contrast transverse view from the CT scan of two patients. The virtual line used to separate valve calcification adjacent to and opposite the MS can be seen running in a roughly 30-45 degree angle to the anterior-posterior axis of the body.



Supplementary figure 2: Study flow diagram.

Supplementary tables

TAVI bioprosthesis type		No Conduction Abnormality (n = 38)	Conduction Abnormality (n = 20)	P value
Balloon-expandable		34 (89.5%)	16 (80%)	0.266
Self-expandable		3 (10.5%)	3 (15%)	
Mechanically-expandable		0 (0%)	1 (5%)	
Pre-TAVI balloon dilatation		10 (26.3%)	10 (50.0%)	0.071
Post-TAVI balloon dilatation		3 (8.1%)	3 (15%)	0.654
Valve size (mm)	20	1 (2.6%)	0 (0.0%)	0.112
	23	12 (31.6%)	5 (25.0%)	
	25	0 (0.0%)	3 (15.0%)	
	26	14 (36.8%)	4 (26.7%)	
	29	10 (26.3%)	8 (40.0%)	
	34	1 (2.6%)	0 (0.0%)	
Valve size (mm)	≤25	13 (34.2%)	12 (40.0%)	N/A
	≥26	25 (65.8%)	20 (60.0%)	

Supplementary table 1: Comparison of TAVI bioprosthesis type between patients with and without CA

Variable	OR	95% CI for OR		P value
		Lower limit	Upper limit	
DLZ calcification adjacent to MS without low δMSID	4	0.299	53.468	0.295
low δMSID without DLZ calcification adjacent to MS	6	0.643	55.948	0.116
low δMSID & DLZ calcification adjacent to MS	36	3.193	405.897	0.004

Supplementary table 2: Univariate logistic regression comparing the association of different combinations of the risk factors for the outcome of post-TAVI conduction abnormality. Low δ MSID defined as <1.25mm. MS- membranous septum, δ MSID- difference between MS and implantation depth, DLZ- device landing zone.